

SEARCH FOR RARE ϕ DECAYS IN $\pi^+\pi^-\gamma$ FINAL STATE

R.R.Akhmetshin, G.A.Aksenov, E.V.Anashkin, M.Arpagaus, V.A.Astakhov,
 B.O.Baibusinov, V.S.Banzarov, L.M.Barkov, A.E.Bondar, D.V.Chernyak,
 S.I.Eidelman, G.V.Fedotovitch, N.I.Gabyshev, A.A.Grebeniuk, D.N.Grigoriev,
 P.M.Ivanov, B.I.Khazin, I.A.Koop, L.M.Kurdadze, A.S.Kuzmin, I.B.Logashenko,
 P.A.Lukin, A.P.Lysenko, A.V.Maksimov, Yu.I.Merzlyakov, I.N.Nesterenko,
 V.S.Okhapkin, E.A.Perevedentsev, E.V.Popkov, T.A.Purlatz, N.I.Root, A.A.Ruban,
 N.M.Ryskulov, M.A.Shubin, B.A.Shwartz, V.A.Sidorov, A.N.Skrinsky, V.P.Smakhtin,
 I.G.Snopkov, E.P.Solodov, A.I.Sukhanov, V.M.Titov, Yu.V.Yudin.
 Budker Institute of Nuclear Physics, Novosibirsk, 630090, Russia

D.H.Brown, B.L.Roberts
 Boston University, Boston, MA 02215, USA

J.A.Thompson, C.M.Valine
 University of Pittsburgh, Pittsburgh, PA 15260, USA

V.W.Hughes
 Yale University, New Haven, CT 06511, USA

Abstract

A search for ϕ radiative decays has been performed using a data sample of about 2.0 million ϕ decays collected by the CMD-2 detector at VEPP-2M collider in Novosibirsk. From the selected $e^+e^- \rightarrow \pi^+\pi^-\gamma$ events the following results were obtained:

$$B(\phi \rightarrow f_0(980)\gamma) < 1 \times 10^{-4} \text{ for destructive and}$$

$B(\phi \rightarrow f_0(980)\gamma) < 7 \times 10^{-4}$ for constructive interference with the Bremsstrahlung process respectively,

$$B(\phi \rightarrow \gamma \rightarrow \pi^+\pi^-\gamma) < 3 \times 10^{-5} \text{ for } E_\gamma > 20 \text{ MeV,}$$

$$B(\phi \rightarrow \rho\gamma) < 7 \times 10^{-4}.$$

From the selected $e^+e^- \rightarrow \mu^+\mu^-\gamma$ events

$$B(\phi \rightarrow \mu^+\mu^-\gamma) = (2.3 \pm 1.0) \times 10^{-5} \text{ has been obtained for } E_\gamma > 20 \text{ MeV.}$$

The upper limit on the P,CP-violating decay $\eta \rightarrow \pi^+\pi^-$ has also been placed:

$$B(\eta \rightarrow \pi^+\pi^-) < 9 \times 10^{-4}.$$

All upper limits are at 90% C.L.

Introduction

The radiative decays of the ϕ meson are accessible at the VEPP-2M collider[1] in Novosibirsk as well as at TJNAF (former CEBAF) [2] and the future Novosibirsk and Frascati ϕ -factories [3, 4]. These decays were studied before (for a review see [5]) and are now under study with SND[6] and CMD-2[7, 8] detectors at VEPP-2M.

The decay $\phi \rightarrow f_0(980)\gamma$ is particularly interesting in two ways:

1) $f_0(980)$ structure. The 20% decay probability into a two kaon final state [9] seems puzzlingly high if $f_0(980)$ is a member of the strangeness-0 scalar meson nonet. Various explanations for this large coupling to kaons have been advanced [10, 11, 12, 13], including the idea that $f_0(980)$ is composed of four quarks, with a "hidden strangeness" component: ($f_0 = s \bar{s}(u \bar{u} + d \bar{d})/\sqrt{2}$), or that it may be a $K - \bar{K}$ molecule. The value of the branching ratio for the $\phi \rightarrow f_0(980)\gamma$ decay mode appears to be very sensitive to the model [10, 14].

2) Possible background to the planned measurement of ϵ'/ϵ at ϕ -factories. The presence in the final state only the $K_S K_L$ from the ϕ decay is of crucial importance for these experiments. The ϕ decay into $f_0(980)\gamma$ accompanied with a low energy photon escaping detection leads to the C-even final state of $K_S K_S$ and can mimic the CP-violating decay. In accordance with [15, 16] this effect becomes significant if the final state has a C-even component as large as 5×10^{-5} . Although theoretical predictions for the probability of this decay give the values about 10^{-6} or even much less [10, 11, 12, 17], the experimental measurement is needed for their confirmation.

The decay $\phi \rightarrow f_0(980)\gamma$ with $f_0(980)$ decaying to two kaons is expected to be too small to be observed with the VEPP-2M collider luminosity because of additional suppression caused by the small differences between the ϕ mass and kaon pair production threshold. But it can be probed through the $f_0(980)$ decay to two charged [18, 19, 20] or two neutral [21] pions. In [14] the branching ratio of the decay $\phi \rightarrow f_0(980)\gamma \rightarrow \pi\pi\gamma$ is predicted at the level of $(1-2) \times 10^{-5}$ in the $K - \bar{K}$ molecule model and 5×10^{-5} for the conventional two quark structure while it is 2.4×10^{-4} in the four-quark model [10]. Thus, observation or even an upper limit for this decay mode will help to distinguish between different possible structures of the $f_0(980)$ meson.

In this paper we present results of a search for the $\phi \rightarrow f_0(980)\gamma$ decay in the event sample where two charged pions and one photon were detected in the CMD-2 detector. The events in our sample arise primarily from the much larger background: the radiative processes $e^+e^- \rightarrow \pi^+\pi^-\gamma$ where the photon comes from initial electrons or from final pions. Therefore the signal from the $f_0(980)\gamma$ final state can be seen most effectively as an interference structure at $E_\gamma \approx 40$ MeV in the spectrum of the photons and depends on the $f_0(980)$ mass (980 ± 10 MeV) and width (40-100 MeV) [9]. Figure 1 presents the photon energy spectra calculated according to the four quark model [14, 22] for three values of the $f_0(980)$ width and three values of the branching ratio. Two parameters of this model were varied to keep the $f_0(980)$ width 40, 70 and 100 MeV. The $f_0(980)$ mass was fixed at 980 MeV. The first column presents a signal for $f_0(980)$ only, while the second and third are the sum of the $f_0(980)$ signal and its interference with the radiative process $e^+e^- \rightarrow \pi^+\pi^-\gamma$ for positive and negative

relative phases. The main contribution from $e^+e^- \rightarrow \pi^+\pi^-\gamma$ (0.03 nb/MeV for 20 MeV photons, falling to 0.015 nb/MeV for 160 MeV photons) is 3 to 10 times higher than the maximum interference signal and is not shown.

The signal was also searched as an interference structure in the energy dependence of the $e^+e^- \rightarrow \pi^+\pi^-\gamma$ cross section.

The CMD-2 Detector

The CMD-2 detector has been described in detail elsewhere [7, 8].

The CsI barrel calorimeter with $6 \times 6 \times 15$ cm³ crystal size covering polar angles from 0.8 to 2.3 radian (892 crystals) is placed outside a 0.4 r.l. superconducting solenoid with a 1 Tesla azimuthally symmetric magnetic field. The endcap calorimeter is made of 680 BGO crystals with $2.5 \times 2.5 \times 15$ cm³ size and was not installed for the data presented here. The drift chamber (DC) inside the solenoid has the momentum resolution of 6% for 500 MeV/c charged particles. The energy resolution for photons in the CsI calorimeter is about 8%. The muon system uses streamer tubes grouped in two layers (inner and outer) with a 15 cm magnet yoke serving as an absorber and has 1-3 cm spatial resolution.

The integrated luminosity of 1480 nb^{-1} collected in 1993 in 14 energy points around the ϕ mass corresponds to the production of about $2.0 \times 10^6 \phi$'s. About 7.2×10^7 events, predominantly beam-beam, beam-gas and Bhabha events were recorded. Some preliminary results from this data set have been published in [23].

Selection of $\pi^+\pi^-\gamma$ Events

The event candidates were selected by a requirement of only two (minimum ionizing) charged tracks in the DC and one or two photons with energy greater than 20 MeV in the CsI calorimeter. Events with invariant mass of two photons close to the π^0 mass were removed. The average momentum of two charged tracks was required to be higher than 240 MeV/c to remove the background from $K_S \rightarrow \pi^+\pi^-$ decays and the radial distance of the closest approach of each track to the interaction region was required to be less than 0.3 cm. The requirement that the Z-coordinate (along the beam) of the vertex be within 10 cm at the detector center reduces cosmic ray background by a factor of two.

The detected photons were required to have a polar angle between 0.85 and 2.25 radians so that they enter the "good" region in the CsI barrel calorimeter.

The detected charged tracks were required to have a polar angle between 1.05 and 2.1 radians so that they enter the inner muon system. The sum of the energy

depositions of two clusters associated with two charged tracks is required to be less than 400 MeV. These cuts removed Bhabha events.

The main background for the $\pi^+\pi^-\gamma$ final state after the above cuts comes from: a) the radiative process $e^+e^- \rightarrow \mu^+\mu^-\gamma$, b) the decay $\phi \rightarrow \pi^+\pi^-\pi^0$ when one of the photons from the π^0 escapes detection, and c) collinear events $e^+e^- \rightarrow \mu^+\mu^-, \pi^+\pi^-$, with a background cluster in the calorimeter from secondary decays and interactions of muons or pions with the detector material.

Selection of Muons

The inner muon system was used to separate muons from pions. The requirement of hits in the inner muon system for both charged tracks selects muon events, together with some pion events in which the products of the nuclear interactions in the calorimeter reach the muon system.

Separation of pion and muon events in the calorimeter is illustrated in Fig. 2, where scatter plots of energy depositions of one track vs. the other one are presented for events with one or no hits in the muon system (a) and selected as muons (b). Energy depositions are corrected for the incident angle. Pions have nuclear interactions and in some cases leave more energy, while muons mostly have only dE/dx losses.

To select a cleaner sample of muon events, in addition to the information from the muon system both tracks were required to show only minimum ionizing energy deposition in the calorimeter (60-130 MeV). All the rest were considered as candidates to pion sample.

The average efficiency of the muon system with above selections was estimated to be $(91\pm 3)\%$. The systematic error is estimated to be about 5% and results in a correlated uncertainty in the selected number of pions and muons.

Simulation of $\pi^+\pi^-\gamma$ events shows that the probability for pions to be selected as muons is about 20% at photon energies below 150 MeV and falls to 5% at 350 MeV photon energy.

Constrained Fit

To reduce the background from collinear events as well as that from three pions a constrained fit was used requiring total energy and momentum conservation (within detector resolution) for a three body decay. About 20% of the selected events had an additional photon. In this case the constrained fit was applied for both possible combinations and the combination with minimum χ^2 was chosen.

Figure 3a presents the $\chi^2/d.f.$ distribution (points with errors) for selected $\pi^+\pi^-\gamma$

events after the above cuts and the constrained fit. The peaked at zero distribution for simulated events of interest is shown as a histogram. The experimental distribution has a "tail" due to the above background processes. This tail is mostly dominated by the three pion events as demonstrated by a flat simulated histogram. A three pion background appears when one of the photons from the π^0 has energy below 20 MeV and is not detected so that the event looks like a three body decay within detector resolution.

The $\chi^2/\text{d.f.}$ distribution for events selected as muons has much less background and is in good agreement with simulation. A cut on the $\chi^2/\text{d.f.}$ less than 3 was imposed.

To obtain the correct number of events and spectra the background subtraction procedure was used. The events with $3 < \chi^2/\text{d.f.} < 6$ were selected to obtain the background spectrum which is shown in Figure 3b (points with errors). The histogram shows the photon spectrum for simulated three pion events with the same cuts. The low energy part of the background spectrum has a big contribution from collinear events. For each energy point the background was subtracted from the events in the region $\chi^2/\text{d.f.} < 3$ used in the further analysis.

As a result of the constrained fit one can obtain an improved estimate for the photon energy. Simulation shows a photon energy resolution about 5 MeV in the whole energy range instead of $\sigma_{E_\gamma} = 8\% \times E_\gamma$ CsI resolution.

In order to extract the resonant contribution associated with the ϕ , two data sets were used. Energy points at $E_{c.m.}$ from 1016 to 1023.2 MeV with the integrated luminosity of 897 nb^{-1} were used for the "phi" region. The points at $E_{c.m.} = 996, 1013, 1026, 1030, 1040$ MeV with the integrated luminosity of 584 nb^{-1} were used for a background estimate from a "non-phi" region, containing 30 times fewer ϕ decays than the "phi" region.

Figures 3c,d present photon spectra corrected by the constrained fit after background subtraction for events with $\chi^2/\text{d.f.} < 3$ for "non-phi" (c) and ϕ (d) regions. Lines present calculated spectra corrected for the detector efficiency (see below).

A peak at 220 MeV corresponds to the radiative process $e^+e^- \rightarrow \rho\gamma$ with the ρ decay into two charged pions. Figure 3d also shows the presence of some background photons with energies higher than 300 MeV presumably coming from the ϕ decay into $\eta\gamma$ with $\eta \rightarrow \pi^+\pi^-\gamma$. If a soft photon from η is not detected, the constrained fit changes the energy of the remaining photon from its 362 MeV peak value within the detector resolution but the $\chi^2/\text{d.f.}$ value remains good. These events are not completely removed by the subtraction procedure.

The region with the photon energy from 20 to 160 MeV has minimum background and has been chosen for the $\phi \rightarrow f_0(980)\gamma$ search.

Figures 3e,f present the same distributions for events selected as muons. Lines are

calculated spectra corrected for the detection efficiency. The presence of pion events in the muon sample is illustrated by the small peak at 220 MeV from ρ decays.

Cross Section Calculation

The cross section for each energy point was calculated as $\sigma = N_{ev}/(L \cdot \epsilon)$.

N_{ev} is the number of selected events with photons having polar angles from 0.85 to 2.25 radians and energy from 20 to 160 MeV and charged particles in the polar angle range 1.05-2.1 radian. The final numbers of muons and pions were corrected for their cross contamination.

The integrated luminosity L for each energy point was determined by Bhabha events with about 2% systematic accuracy.

The detection efficiency ϵ was obtained by simulation. The CsI single photon efficiency is about 80% for 20 MeV photons and reaches 100% level above 70 MeV. The $\pi^+\pi^-\gamma$ and $\mu^+\mu^-\gamma$ detection efficiency decreases with photon energy increase because the acceptance is higher for nearly collinear tracks and is on the average 20%. The center of mass energy, integrated luminosity for each energy point, the number of selected events with pions and muons and corresponding cross sections are presented in Table 1. The errors of the cross sections are statistical only. The systematic error in the experimental cross sections was estimated to be about 6% dominated by the uncertainty of the muon system efficiency.

Determination of the Branching Ratios

The obtained cross sections of the processes $e^+e^- \rightarrow \pi^+\pi^-\gamma$ and $e^+e^- \rightarrow \mu^+\mu^-\gamma$ versus energy are presented in Fig. 4a,b. To interpret the data we follow the model described in [22]. The resulting cross section (the formula for its energy dependence is not presented here because of its cumbersomeness) contains contributions from different reactions: Bremsstrahlung by initial and final particles as well as the direct hadronic decay $\phi \rightarrow \pi^+\pi^-\gamma$.

The process of Bremsstrahlung from initial particles is suppressed by selecting photons transverse to the beam direction, but it still accounts for 2/3 of the $e^+e^- \rightarrow \pi^+\pi^-\gamma$ and one half of the $e^+e^- \rightarrow \mu^+\mu^-\gamma$ cross section.

Also taken into account is the ϕ contribution to the photon propagator (vacuum polarization). This contribution gives rise to an interference pattern in the cross section at the ϕ mass and can be referred to as a "radiative" decay $\phi \rightarrow \gamma \rightarrow \pi^+\pi^-\gamma$. The amplitude of the interference is determined by the ϕ -meson leptonic width. The same is valid for the $\mu^+\mu^-\gamma$ final state.

The direct hadronic decay $\phi \rightarrow \pi^+\pi^-\gamma$ is expected to be dominated by the $\phi \rightarrow f_0(980)\gamma$ decay. If the amplitude of this process is high enough, the interference pattern in the cross section is predicted to be different from that with the vacuum polarization contamination only.

To fit our data the calculations performed in [22] were used in the case when $f_0(980)$ is a four quark state. The four quark model predicts for the branching ratio $B(\phi \rightarrow f_0(980)\gamma)=2.4 \times 10^{-4}$, close to the sensitivity of our experiment while the two quark and kaon molecule models predict values below our sensitivity and were not used for fitting.

Using the above descriptions the following results have been obtained:

1. If direct hadronic decays of the ϕ give no contribution to the observed $\pi\pi\gamma$ events, the fit with only hadronic vacuum polarization pattern gives:

$$B(\phi \rightarrow \pi^+\pi^-\gamma) < 3.0 \times 10^{-5} \text{ at } 90\% \text{ CL,}$$

$$B(\phi \rightarrow \mu^+\mu^-\gamma)=(2.3 \pm 1.0) \times 10^{-5}.$$

The present upper limit for the first decay is $B(\phi \rightarrow \pi^+\pi^-\gamma) < 7 \times 10^{-3}$ [24] while there are no other measurements for the $B(\phi \rightarrow \mu^+\mu^-\gamma)$. These results correspond to the photon energy $E_\gamma > 20$ MeV and don't contradict to the theoretical calculations for these processes [22]:

$$B(\phi \rightarrow \pi^+\pi^-\gamma)=4.74 \times 10^{-6},$$

$$B(\phi \rightarrow \mu^+\mu^-\gamma)=1.15 \times 10^{-5}.$$

For the experimental range of angles and photon energies, the ratio σ_{exp}/σ_{th} for pions and muons is 0.95 ± 0.05 and 0.98 ± 0.04 respectively showing good agreement with theory. Theoretical predictions with the ϕ -meson leptonic width from [9] are shown in Fig. 4a (solid line) and Fig. 4b, the $\chi^2/d.f.$ are 7.4/10 and 4.8/10 respectively.

2. Taking the value of the leptonic width from [9], we are fixing the vacuum polarization contribution to the decay $\phi \rightarrow \pi^+\pi^-\gamma$. After that the following upper limits for $f_0(980)\gamma$ production have been obtained from the c.m. energy dependence of the cross section and two different signs of the interference at 90% CL:

$$B(\phi \rightarrow f_0(980)\gamma) < 10 \times 10^{-4} \text{ for " +",}$$

$$B(\phi \rightarrow f_0(980)\gamma) < 4 \times 10^{-4} \text{ for " -".}$$

The results above correspond to all possible photon energies. The predicted cross sections in the case of the four quark model are presented in Fig. 4a for two signs of

relative phases.

The signal from the decay of the $\phi \rightarrow f_0(980)\gamma$ would be also seen as a structure in the radiative differential photon spectra from the "phi" region. These spectra are shown in Fig. 5 for six c.m.energy points for photons in the 20-160 MeV energy range. The spectra were corrected for all experimental inefficiencies and normalized to the integrated luminosity. Also shown is the theoretical prediction from the four quark model [22, 14] for two possible signs of interference.

The above spectra were fit as a group, with the photon spectrum calculated for each energy point taking into account the uncertainties in the $f_0(980)$ mass and width. As a result, lower upper limits have been obtained at 90% CL:

$$\begin{aligned} B(\phi \rightarrow f_0(980)\gamma) &< 7 \times 10^{-4} \text{ for "+"}, \\ B(\phi \rightarrow f_0(980)\gamma) &< 1 \times 10^{-4} \text{ for "-"} . \end{aligned}$$

Search for $\phi \rightarrow \rho\gamma$ Decay

The selected $\pi^+\pi^-\gamma$ events with photon energies from 100 to 300 MeV (see Fig. 3d) can be used to search for the C violating decay $\phi \rightarrow \rho\gamma$ with the ρ decay into two charged pions. The cross section vs. energy for the events with photons in the 100-300 MeV range is presented in Fig. 6. The fit of the energy dependence of the cross section by the theoretical calculation [22] gives the ratio $\sigma_{exp}/\sigma_{th}=1.04\pm 0.05$ and shows that maximum possible signal from the ϕ does not exceed 1.7 nb at 90% C.L. It corresponds to the following upper limit:

$$B(\phi \rightarrow \rho\gamma) < 7 \times 10^{-4} \text{ at 90\% C.L.}$$

which is thirty times better than the previous one [25].

Search for $\eta \rightarrow \pi^+\pi^-$ Decay

The selected $\pi^+\pi^-\gamma$ events can be used to search for the P and CP violating decay $\eta \rightarrow \pi^+\pi^-$, where the η comes from the radiative $\phi \rightarrow \eta\gamma$ decay. This decay should be seen as a narrow peak at the photon energy of 362 MeV.

With 897 nb^{-1} in the "phi" region the total number of produced η was estimated as 26900 and can be used for normalization.

As mentioned above, the constrained fit procedure improves the photon energy resolution to about 5 MeV. Figure 7 demonstrates this improvement where simulated

photon spectra are shown by histogram before and after (shaded) constrained fit. The experimental spectrum for the " ϕ " region is shown by points with errors. Only background events are seen in the 362 MeV region and the number of possible $\eta \rightarrow \pi^+\pi^-$ events was estimated to be $N < 4$.

The detection efficiency for these events taken from simulation is $(16\pm 3)\%$. The corresponding upper limit is:

$$B(\eta \rightarrow \pi^+\pi^-) < 9 \times 10^{-4} \text{ at } 90\% \text{ C.L.},$$

which is a factor of 1.5 better than the only existing one from [26].

Conclusions

Using about 30% of available data at the ϕ -meson the selection of $e^+e^- \rightarrow \pi^+\pi^-\gamma$ and $e^+e^- \rightarrow \mu^+\mu^-\gamma$ events was performed. A new upper limit for the $\phi \rightarrow f_0(980)\gamma$ decay has been obtained

$$B(\phi \rightarrow f_0(980)\gamma) < (1 - 7) \times 10^{-4} \text{ at } 90\% \text{ C.L.}$$

depending on the sign of interference with the radiative process $e^+e^- \rightarrow \pi^+\pi^-\gamma$. This result can be compared with the only existing $B(\phi \rightarrow f_0(980)\gamma) < 2 \times 10^{-3}$ [5].

Assuming that the contribution of the direct hadronic decay of ϕ into $\pi^+\pi^-\gamma$ is negligible, the following result has been obtained:

$$B(\phi \rightarrow \gamma \rightarrow \pi^+\pi^-\gamma) < 3 \times 10^{-5} \text{ at } 90\% \text{ C.L. and } E_\gamma > 20 \text{ MeV}$$

which should be compared with $B(\phi \rightarrow \pi^+\pi^-\gamma) < 7 \times 10^{-3}$ obtained in [24].

The result

$$B(\phi \rightarrow \gamma \rightarrow \mu^+\mu^-\gamma) = (2.3 \pm 1.0) \times 10^{-5}$$

for photon energies $E_\gamma > 20 \text{ MeV}$ is obtained for the first time.

For the C violating decay of $\phi \rightarrow \rho\gamma$ and P,CP violating decay of $\eta \rightarrow \pi^+\pi^-$ the following results have been obtained:

$$B(\phi \rightarrow \rho\gamma) < 7 \times 10^{-4} \text{ at } 90\% \text{ C.L.},$$

$$B(\eta \rightarrow \pi^+\pi^-) < 9 \times 10^{-4} \text{ at } 90\% \text{ C.L.}$$

which are also better than previous ones [25, 26].

Analysis of the collected data is in progress and we expect new results on the ϕ rare decays.

Acknowledgements

The authors are grateful to N.N.Achasov and V.V.Gubin for useful discussions and help with the data interpretation.

This work is supported in part by the US Department of Energy, US National Science Foundation and the International Science Foundation under the grants RPT000 and RPT300.

M.Arpagaus acknowledges support from the Swiss National Science Foundation.

References

- [1] V.V.Anashin *et al.*, Preprint INP 84-114, Novosibirsk, 1984.
- [2] H.Crannell *et al.*, Preprint PR-94-016, CEBAF, 1994.
- [3] A.N.Skrinsky, Proceedings of the Workshop on Physics and Detectors for DAΦNE, Frascati, April 1991, p. 67.
- [4] G.Vignola, Proceedings of the Workshop on Physics and Detectors for DAΦNE, Frascati, April 1991, p. 11.
- [5] S.I.Dolinsky *et al.*, Phys. Rep. **202** (1991)99.
- [6] V.M.Aulchenko *et al.*, Preprint BudkerINP 95-56, Novosibirsk, 1995.
- [7] G.A.Aksenov *et al.*, Preprint BudkerINP 85-118, Novosibirsk, 1985.
- [8] E.V. Anashkin *et al.*, ICFA Instrumentation Bulletin **5** (1988) 18.
- [9] R.M.Barnett *et al.*, Phys.Rev.**D54**(1996)1.
- [10] N.N.Achasov and V.N.Ivanchenko, Nuclear Physics **B315**(1989) 465.
- [11] S.Nussinov and Tran N. Truong, Phys. Rev. Lett. **63**(1989)1349; A.A. Pivovarov, Soviet Physics - Lebedev Institute Reports **9**(1990) 12; N. Paver, contribution to the ϕ Factory Workshop at UCLA, April, 1990.; J.L. Lucio and J.Pestieau, Phys. Rev. **D42**(1990)3253; S. Fajfer and R.J. Oakes, Phys. Rev. **D42**(1990)2392.
- [12] F. Close, Proceedings of the Workshop on Physics and Detectors for DAΦNE, Frascati, April 1991, p.309; F.E. Close, N. Isgur, and S. Kumano, Nucl. Phys.**B389** (1993) 513.
- [13] R. Baldini Ferroli, Proceedings of the Workshop on Physics and Detectors for DAΦNE, Frascati, April 1991, p.665; L.Maiani, *ibid* p.719; N.N.Achasov, *ibid* p.421; M.R.Pennington, *ibid* p.361.
- [14] N.N.Achasov and V.V.Gubin, Preprint IM SB RAS 1-97, Novosibirsk, Russia; hep-ph/9703367, 19 March 1997. Will be published in Phys. Rev. **D**

- [15] D.Cocolicchio *et al.*, Phys. Lett. **B238** (1990) 417.
- [16] P. Franzini, Proceedings of the Workshop on Physics and Detectors for DAΦNE, Frascati, April 1991, p.733.
- [17] J.L. Rosner, I. Dunietz, J. Hauser, Phys. Rev. **D35** (1987) 2166.
- [18] S. Eidelman, E. Solodov, and J. Thompson, Nuclear Physics B (Proceedings Supplement) **24A** (1991) 174.
- [19] S. Eidelman, J.A.Thompson and C.H.Yang, Proceedings of the Workshop on Physics and Detectors for DAΦNE, Frascati, April 1991, p. 437.
- [20] P.J.Franzini, W.Kim and J.Lee-Franzini, Phys. Lett. **B287** (1992) 259; A.Bramon, G.Colangelo and M.Greco, Phys. Lett. **B287** (1992)263.
- [21] J.Lee-Franzini, W.Kim and P.J.Franzini, LNF Preprint 92-025 (P), Frascati, 1992.
- [22] N.N.Achasov, V.V.Gubin and E.P.Solodov, Phys. Rev. **D55** (1997) 2672.
- [23] R.R.Akhmetshin *et al.*, Preprint BudkerINP 95-62, Novosibirsk, 1995.
- [24] G.Cosme *et al.*, Phys. Lett. **B48** (1974) 155.
- [25] J.S.Lindsey *et al.*, Phys. Rev. **147** (1966) 913.
- [26] J.J.Thaler *et al.*, Phys. Rev. **D7** (1973) 2569.

Table 1: Energy, Integrated luminosity, Number of Events and Experimental Cross Sections for $\pi^+\pi^-\gamma$ and $\mu^+\mu^-\gamma$ Channels.

$E_{c.m.}, \text{ MeV}$	$L, \text{ nb}^{-1}$	$N_{\pi^+\pi^-\gamma}$	$N_{\mu^+\mu^-\gamma}$	$\sigma_{\pi^+\pi^-\gamma}, \text{ nb}$	$\sigma_{\mu^+\mu^-\gamma}, \text{ nb}$
994.000±0.600	152.0±0.6	122±13	74±10	3.30±0.35	1.91±0.26
1012.734±0.076	110.9±0.5	52± 9	76±10	1.92±0.36	2.00±0.35
1016.546±0.068	85.5±0.5	48± 9	44± 8	2.18±0.42	2.08±0.36
1018.585±0.340	204.3±0.7	87±14	103±12	1.68±0.29	2.03±0.23
1019.566±0.062	102.0±0.5	45±10	48± 8	2.06±0.44	2.07±0.33
1020.676±0.062	89.1±0.5	37± 9	43±12	1.79±0.39	1.94±0.38
1021.519±0.121	203.2±0.6	117±14	128±13	2.27±0.28	2.56±0.24
1022.638±0.372	212.4±0.6	99±14	136±10	1.89±0.27	2.56±0.24
1025.586±0.070	117.9±0.5	61± 9	72±10	2.09±0.33	2.42±0.32
1029.402±0.064	121.7±0.6	40± 9	55± 8	1.46±0.33	1.99±0.30
1040.000±0.600	81.8±0.5	35± 8	45± 7	1.76±0.39	2.18±0.35

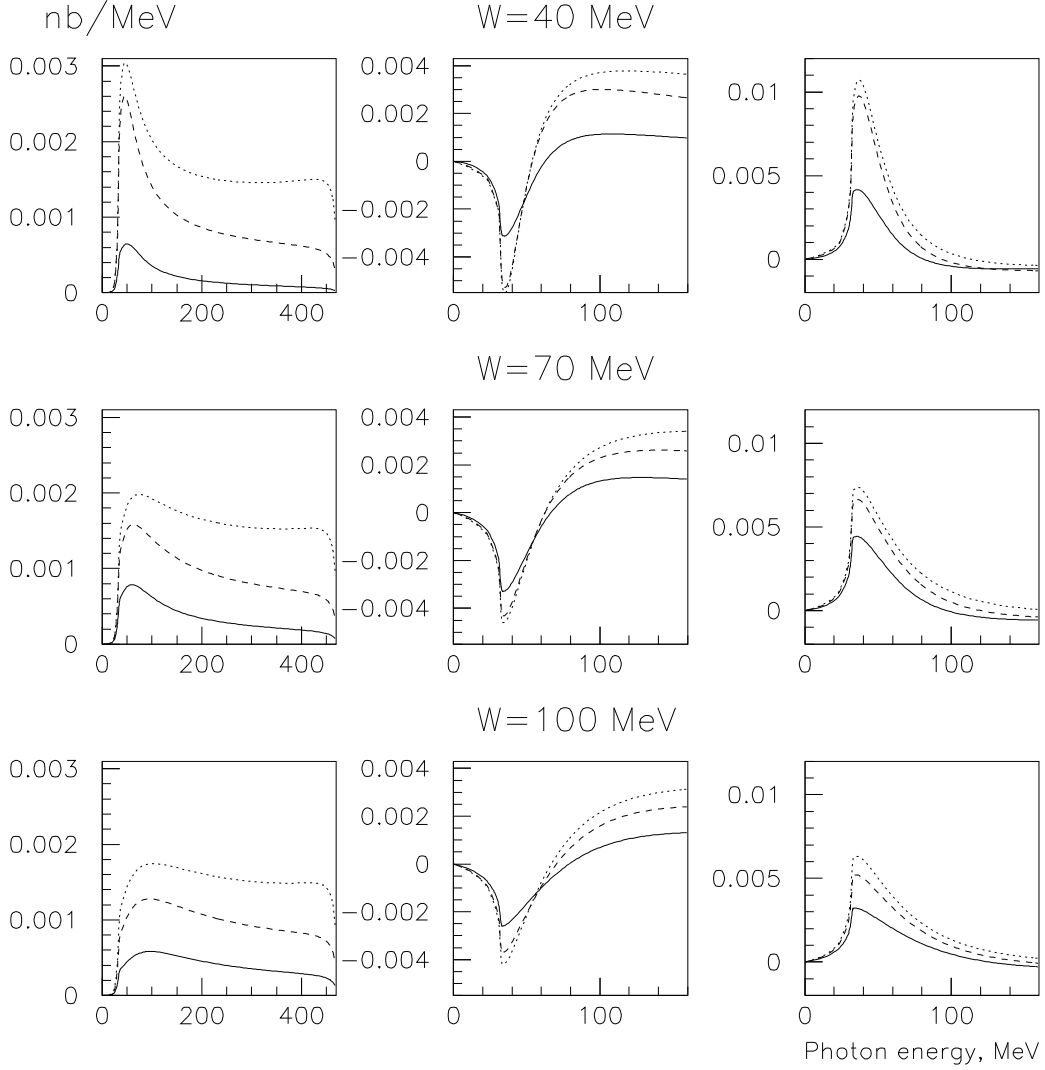


Figure 1: The signal from $\phi \rightarrow f_0(980)\gamma$ decay in the photon spectra in the case of the four quark model for the $f_0(980)$ width of 40, 70 and 100 MeV and three values of branching ratios - 1, 3, 5×10^{-4} (solid, dashed and dotted lines respectively). The first column is for the f_0 signal only, the second and third are the sum of the f_0 signal and interference of f_0 with the radiative process $e^+e^- \rightarrow \pi^+\pi^-\gamma$ with positive and negative relative phase. The main contribution from $e^+e^- \rightarrow \pi^+\pi^-\gamma$ is not shown.

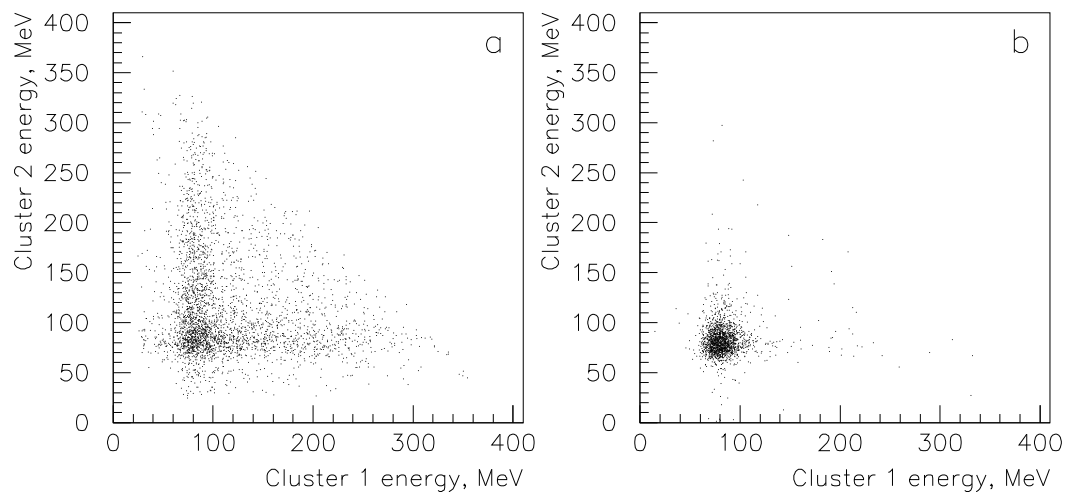


Figure 2: Calorimeter response for events with 1 or no hits in the muon system (a) and for events selected as muons (b).

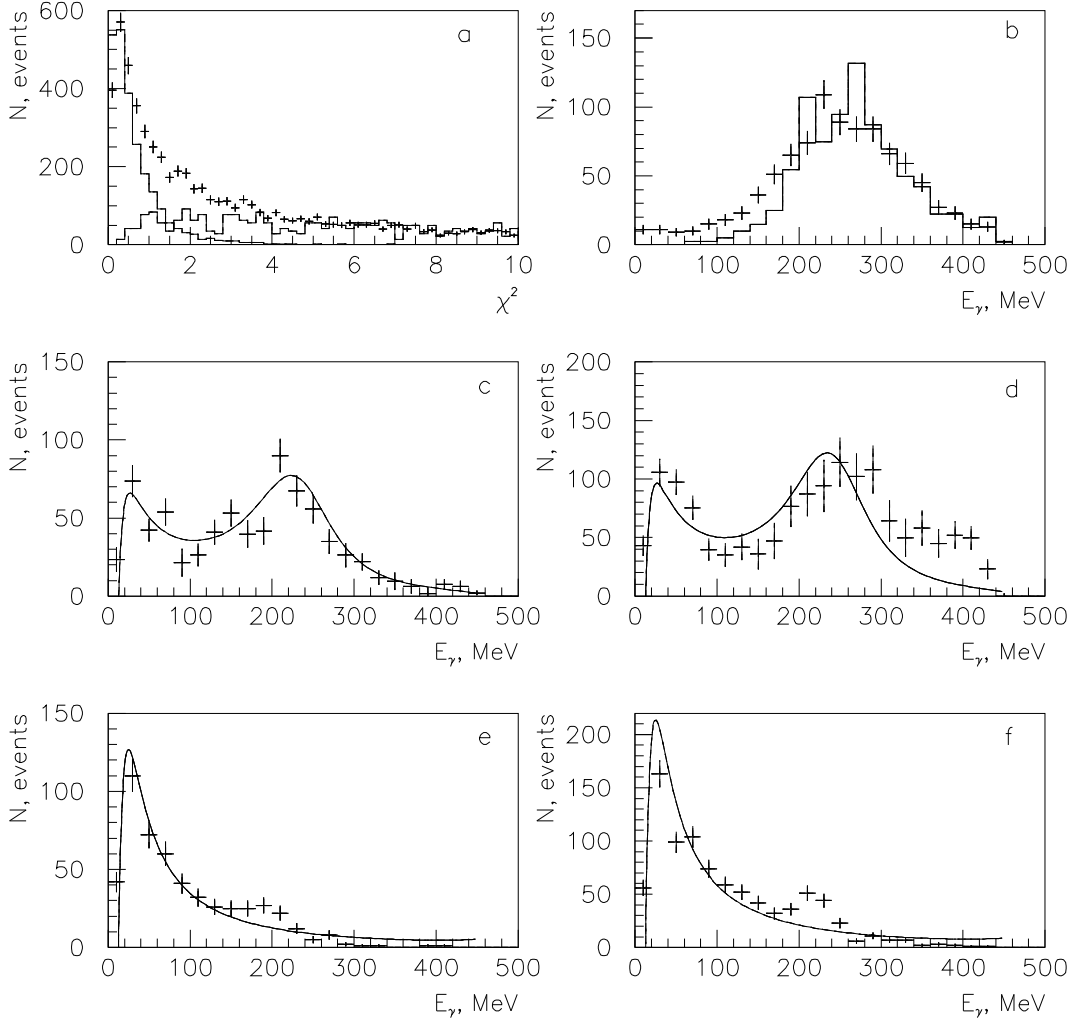


Figure 3: Event selection. a- $\chi^2/\text{d.f.}$ distribution for events (dots with errors) and simulation(histograms); b-photon energy spectrum for background events (histogram is for 3 pion simulation); c,d-photon energy spectra for $\pi^+\pi^-\gamma$ events after background subtraction for the "non- ϕ " region (c) and " ϕ " region (d) (lines are calculation); e-f - the same photon energy spectra for $\mu^+\mu^-\gamma$ events.

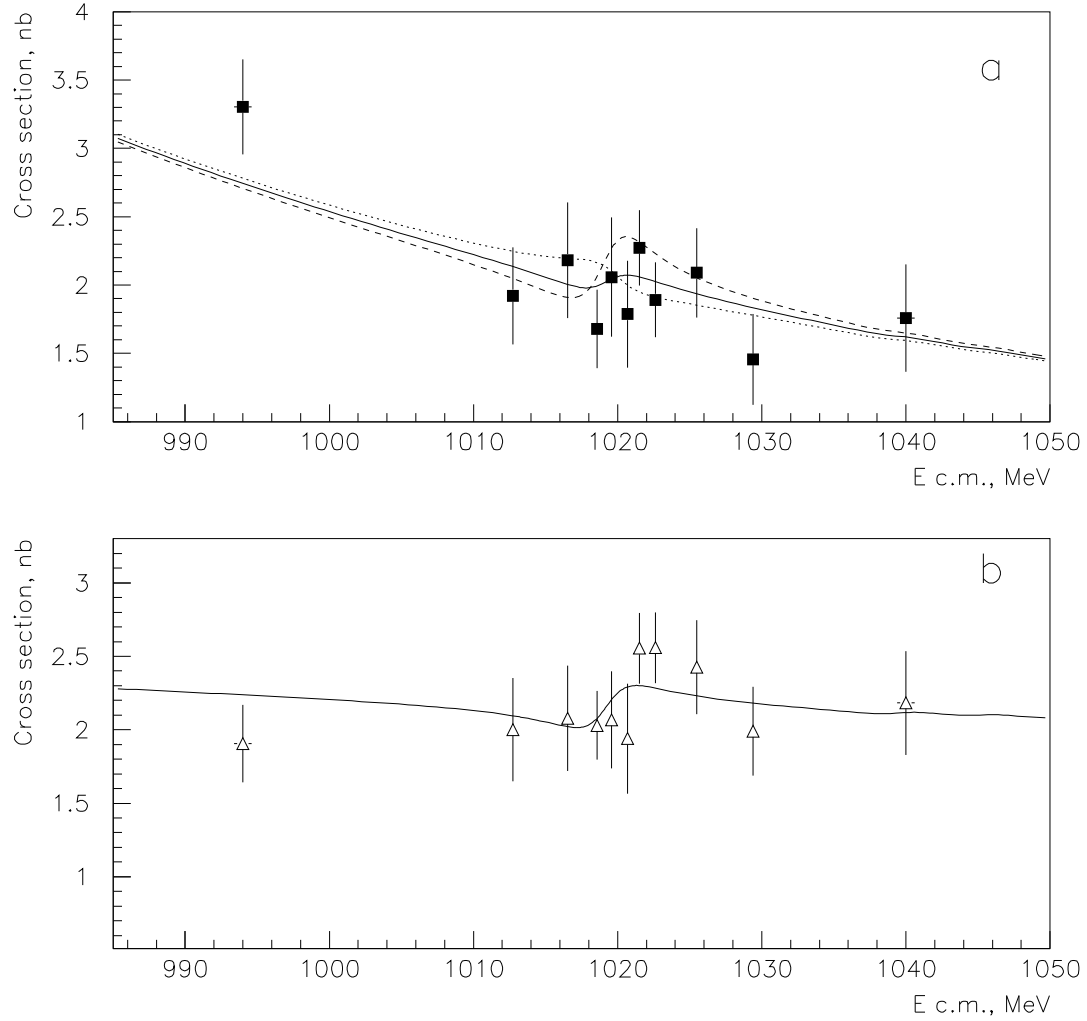


Figure 4: $\phi \rightarrow f_0(980)\gamma$ search: a. The cross section for $e^+e^- \rightarrow \pi^+\pi^-\gamma$. Lines are theoretical predictions in case of no $f_0(980)\gamma$ signal (solid line), $f_0(980)\gamma$ signal with $B(\phi \rightarrow f_0\gamma) = 2.4 \times 10^{-4}$ for the positive (dashed line) and negative relative phase (dotted line); b. The cross section for $e^+e^- \rightarrow \mu^+\mu^-\gamma$ with the theoretical prediction.

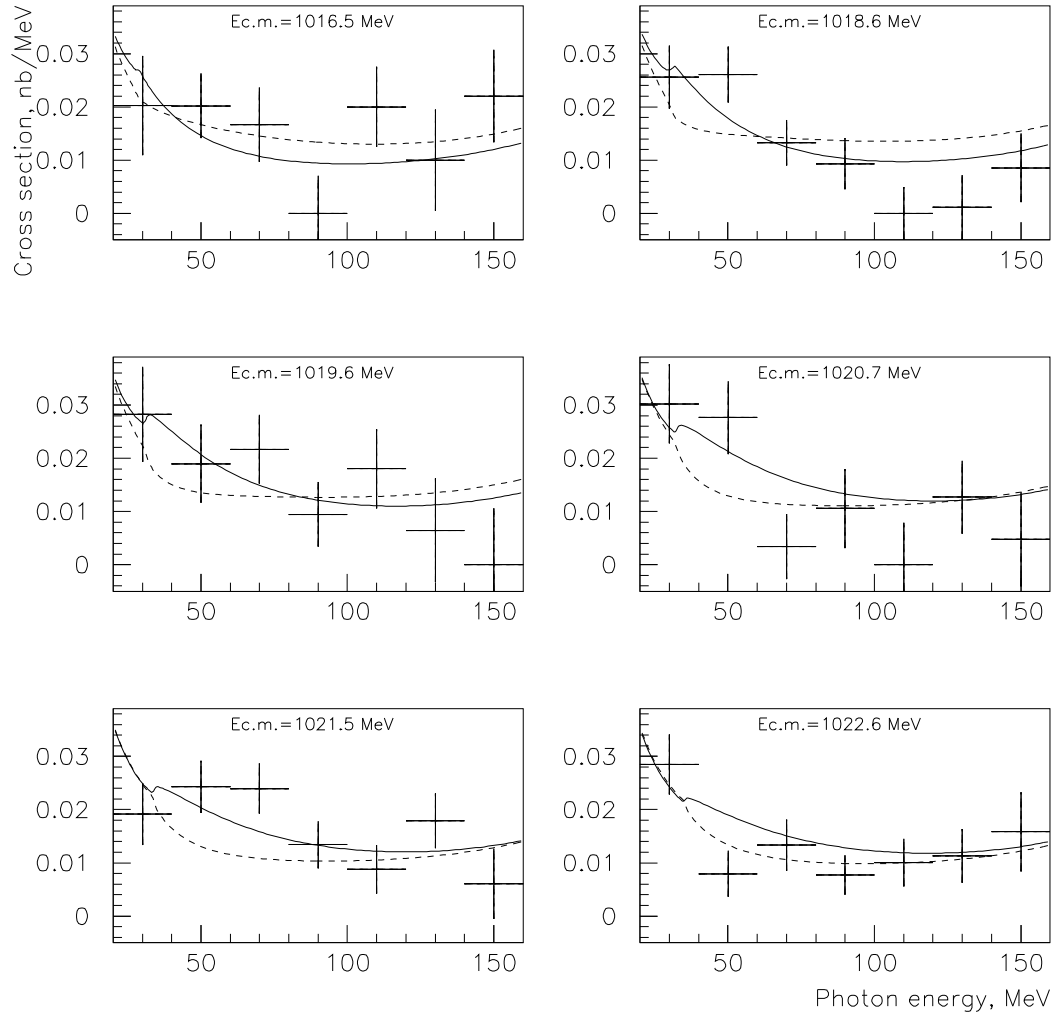


Figure 5: $\phi \rightarrow f_0(980)\gamma$ search: Photon spectra for six c.m.energy point in the " ϕ " region. Lines are theoretical predictions for the four quark model for the branching ratio of 2.4×10^{-4} in the case of the positive (solid line) and negative (dashed line) interference sign and a 70 MeV $f_0(980)$ width.

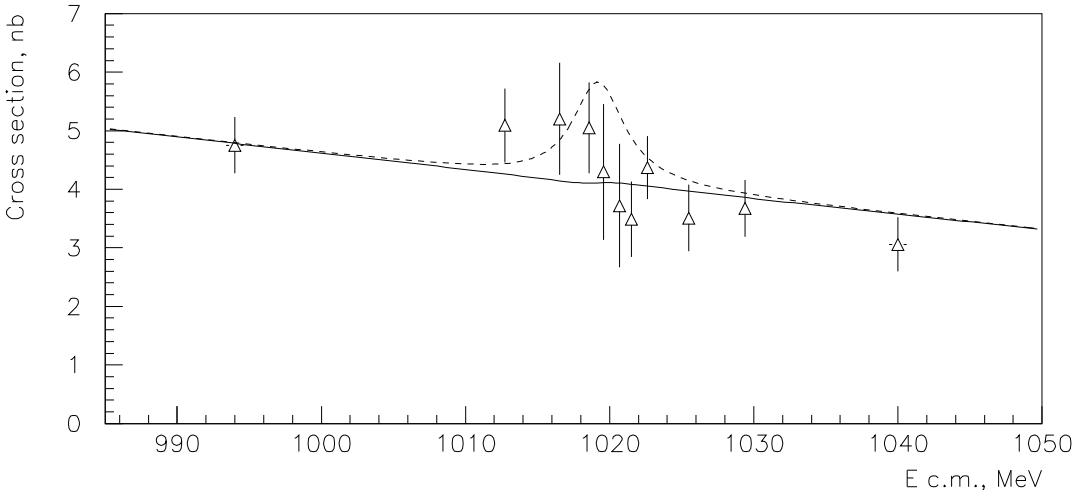


Figure 6: $\phi \rightarrow \rho\gamma$ search. The cross section for $\pi^+\pi^-\gamma$ events for photons in the 100-300 MeV region. The solid line is the theoretical prediction. The dashed line shows the possible ϕ signal at 90% C.L.

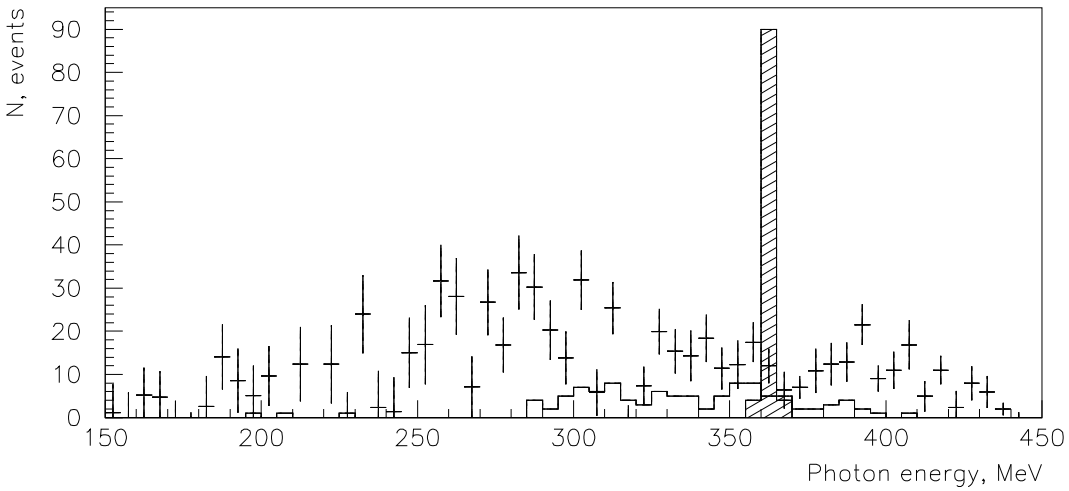


Figure 7: $\eta \rightarrow \pi^+\pi^-$ search. The experimental photon spectrum for for $\pi^+\pi^-\gamma$ events from " ϕ " region. Histograms are simulation of the $\eta \rightarrow \pi^+\pi^-$ decay before and after (shaded) constrained fit.